Targeted Nr2e3 gene region contains Exon 1 and Exon 2

GGATCATACACTGTGTCCAGCGCTGTGCTGGCAGAAGTCTGGACCCAGAGCCAGGGTGGTGAAA
CGCTTCAGAAGGAAGAAACGCTCCTAACTTACAAGGCAAGGGAAGTAGAGGAGAGACAGGCACAG
ACTGAAAGACAGACAGACAGACAGACAGGGGTTAAAGATGGATGCATCGGTTGGGCCCAGCAACT
TCTAGCAAGCAGGCTACCCTTAGGACCATCCATATCCGATGAGCTCTACAGTGGCTGCCTCCACTA
TGCCTGTGTCTGTGGCGGCCTCCAAGAAGGAGTCTCCAGGTAGA***TGGGGCCTTGGAGAGGATCC***
AACAGGTATGATTTTTCTGGAGGTGTGGTCTGGACCTTTGAGGAAGAGAGTGTAACAGTAGGTTC
AGAGAGCCACGAGCGAGCTTGAGCCACATAGCCCCAACCCCAGGGCTGTGAGCAAGCATGAGA
GTCTGCTGGCAACCCCAGAGTCCTAGAAACTGAGAGGCCAGCAGAGCAAGACCCAACAACTGG
CTGCTGAGGCAGGAAATGGGTGCTCTTGAGACACAGAGAGATCTCGAGAGAGGCTGCAGCCGC
CCATAGGGGAGGAATGGGGCTGGGAAGGTGGAAGCCATGGAGGGAAAAGAGAGGGGAAGGG
GTGGGAGCAGAGGTTAGGATGCCACAGTGAGGAAGCTGCTGTTTCCGGTGGGAGTCACATGGG
CAGATCTAGTTTGAGGAACGTGGGAACCTATGGACCGGAGGGAAAGGGGGTGACTAGGGGAGG
GAGTGGGGAGCTATCTCAGTTCAGCCCTGCCTTCTTGCTCAGGTGTGGGCCCCTCGCTCCAGTG
CCGAGTGTGTGGGACAGCAGCAGTGGGAAACATTATGGCATCTATGCCTGCAATGGCTGCAGTG
GCTTCTTCAAGAGGAGTGTGAGAAGGAGGCTCATCTACAGGTGCCACAGCTCTGCCGGCCTGCCC
CGGTGTGCCTAGCACGGGTGGAGGGCGTTCAGGGAAAGCGGAAGACGAGACCAGGGCAAACATA
TCCCAAGTCAAGGCCTAGAGTCAGGGCATGACACTGCCCCCCCAGGAGCTCGTGTCCTCTGCAG

Supplementary Figure 1. NR2E3 gene ablation *in vivo* using CAS9/CRIPSR gene editing system. The sequence of NR2E3 gene exon 1 and exon 2 included intron sequence. The PAM sites are shown (undelined). The 519 bp deletion region is indicated (bold type).

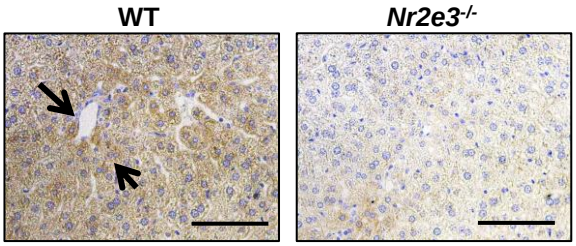

Supplementary Figure 2. Expression of NR2E3 protein in hepatocytes. Representative images of NR2E3 immunostaining in the liver tissues of WT (top) vs. *Nr2e3*$^{-/-}$ KO (bottom) mice. Long arrows indicates central vein while short arrows indicate pericentral hepatocytes. Scale bar represents 100 μm.

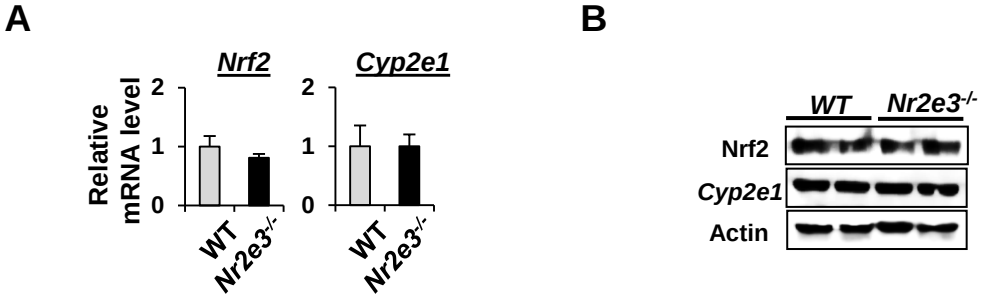

Supplementary Figure 3. Effects of NR2E3 ablation in vivo on gene expression level changes. No changes in mRNA (A) and protein levels (B) of Nrf2, p53, and Cyp2e1 between the liver tissues of WT and *Nr2e3*$^{-/-}$ KO mice. Values are represented as mean ± SD.

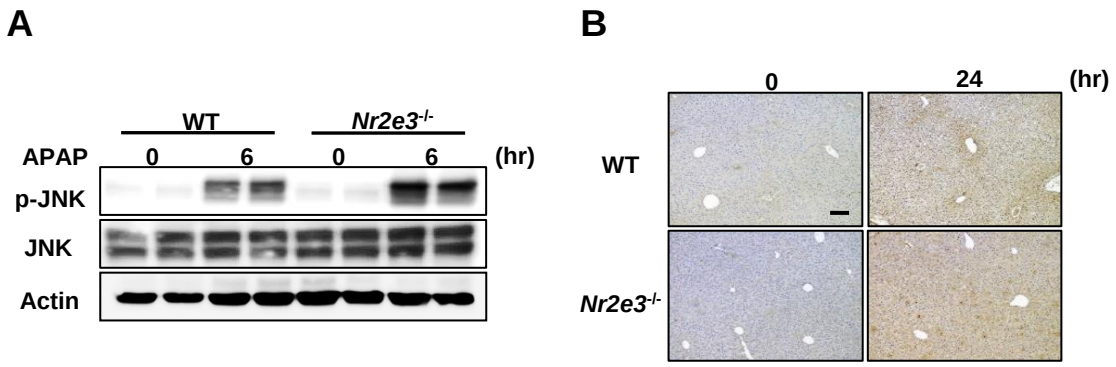

Supplementary Figure 4. Effects of NR2E3 ablation *in vivo* on the status of JNK phosphorylation (A) and the formation of peroxynitrite (B) by APAP treatment. Significantly increased JNK phosphorylation and b nitrotyrosine formation were observed in *Nr2e3*$^{-/-}$ KO mice treated with APAP. Scale bar 100 μm.

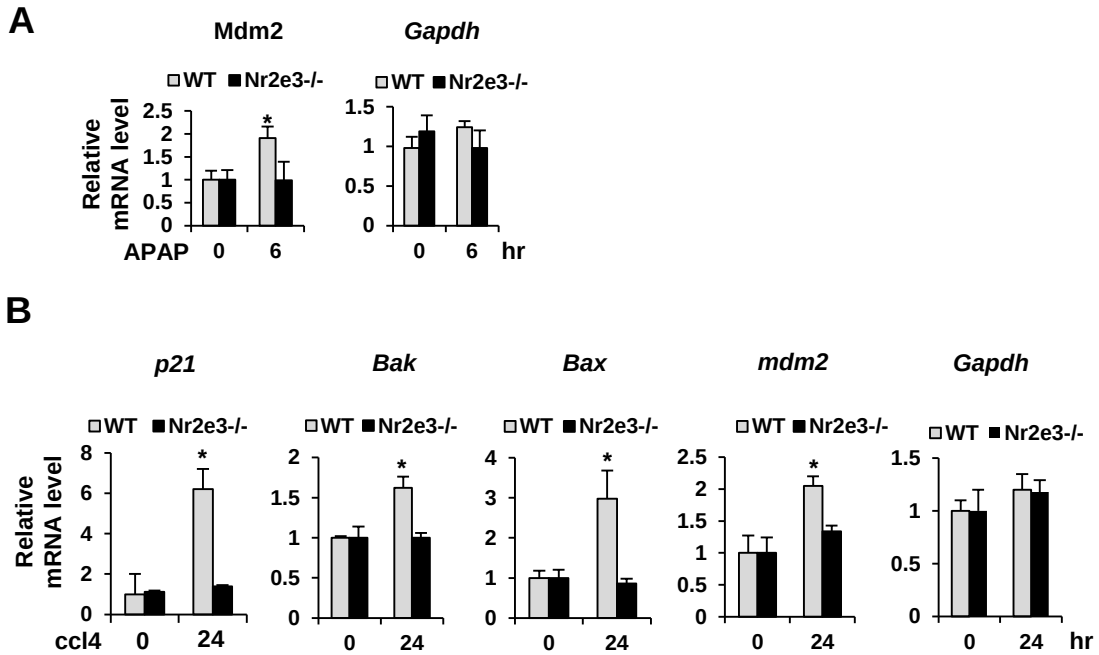

Supplementary Figure 5. Effects of NR2E3 ablation in vivo on p53 downstream target gene expressions in APAP- (A) and ccl4-inducedliver injury (B). Gapdh gene was used as a negative control. Values are represented as mean ± SD. *Significant induction P < 0.05.

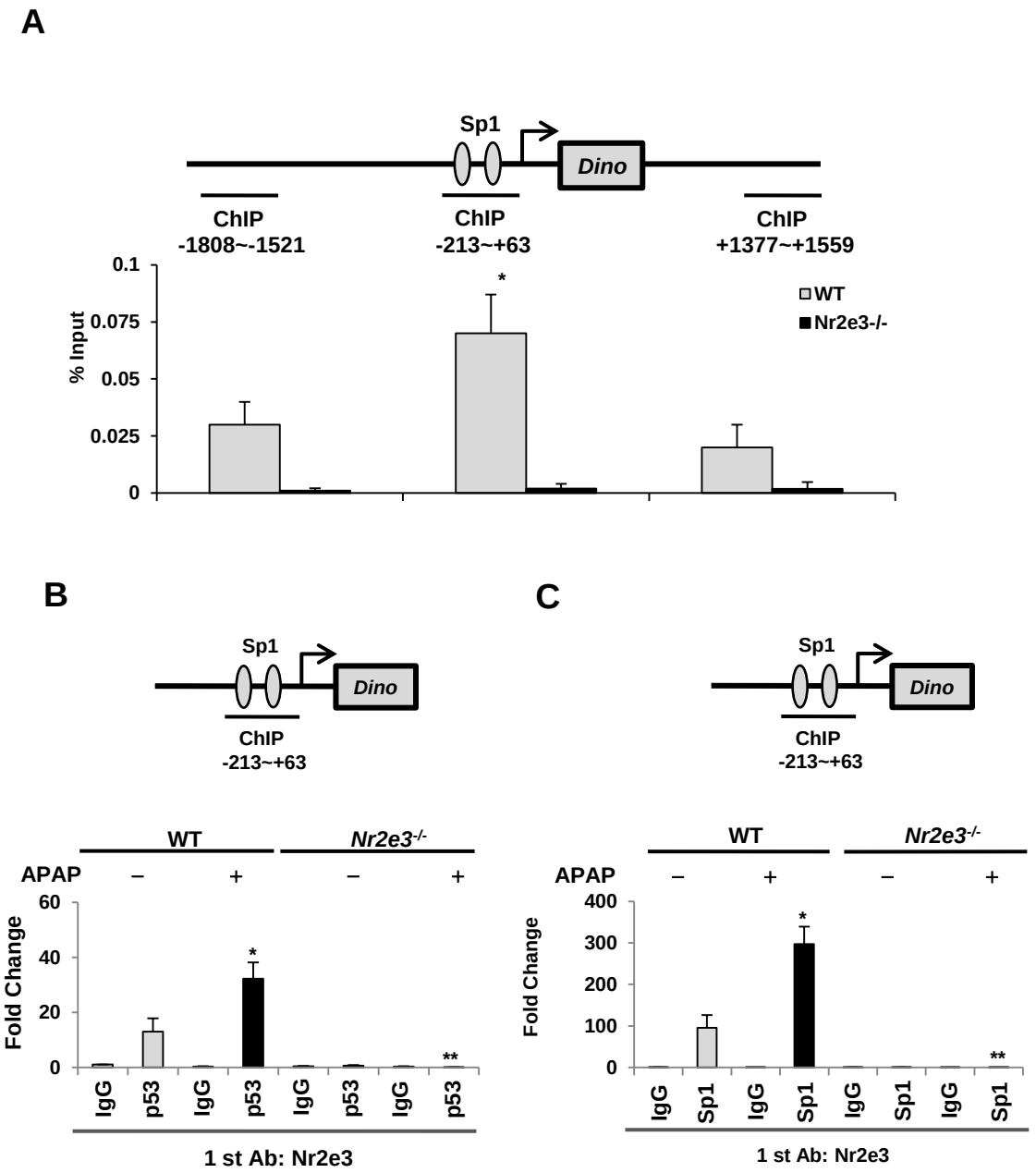

Supplementary Figure 6. Roles of NR2E3 in p53 and RNA pol II recruitment to DINO proximal gene promoter region. (A and B) The results from ChIP assays indicated that there was enhanced NR2E3–p53 and NR2E3–Sp1 complex formation in the DINO gene proximal region in the APAP-treated liver tissues of WT mice, but not in the absence of NR2E3. Consensus Sp1 binding sequences are shown as oval shapes. Values are represented as mean ± SD. *Significant induction or **repression $P < 0.05$.

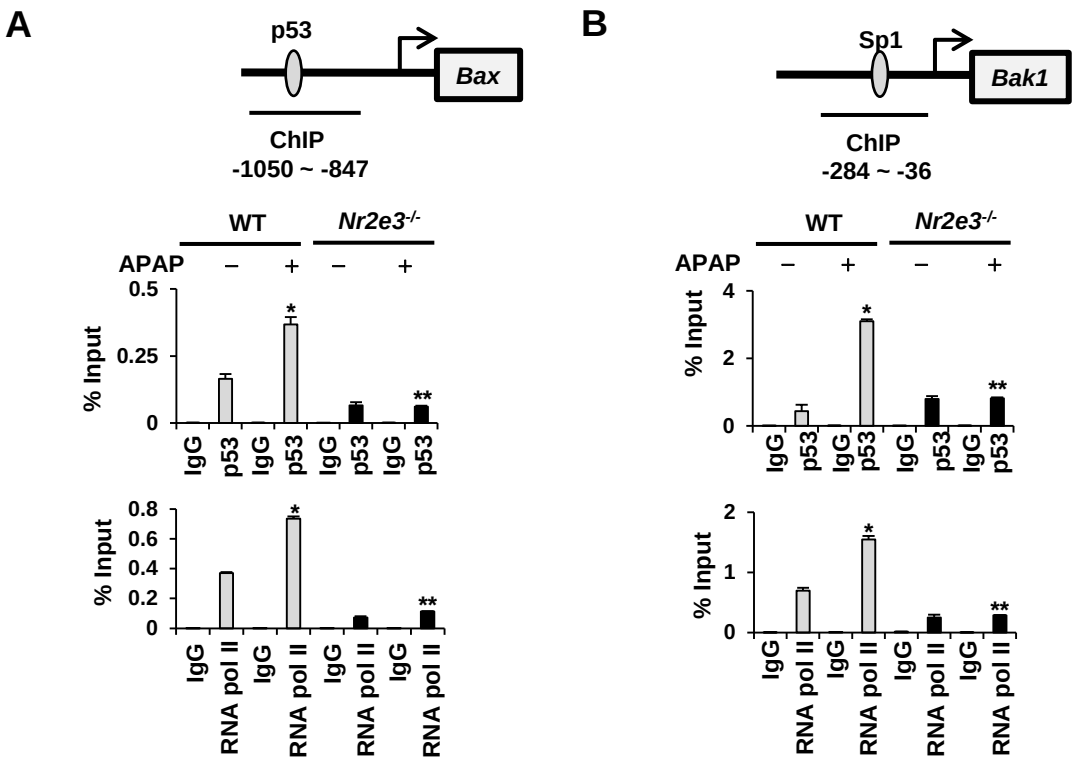

Supplementary Figure 7. Roles of NR2E3 in p53 and RNA pol II recruitment to p53 target gene promoters. (A and B) The recruitment of p53 and RNA pol II to the promoter regions of Bax and Bak1, major p53 downstream target genes, was severely impaired after APAP treatment (6 hr) in the absence of NR2E3 *in vivo*. The consensus p53 binding or Sp1 binding sequence is indicated by oval shape. Values are represented as mean ± SD. *Significant induction or **repression $P < 0.05$.

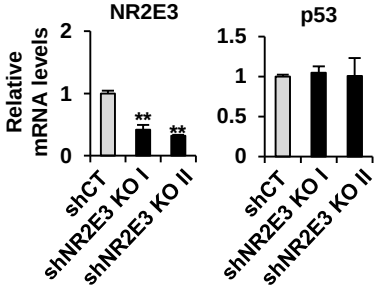

Supplementary Figure 8. Effects of NR2E3 depletion on NR2E3 and p53 mRNA levels. NR2E3 proteins were depleted in HepG2 cells using small hairpin (sh) RNAs targeting NR2E3 (shNR2E3 I and II) with scrambled control (shCT). NR2E3 depletion reduced NR2E3 mRNA levels but did not affect p53 basal mRNA levels. Values are represented as mean ± SD. **Significant reduction $P < 0.05$.

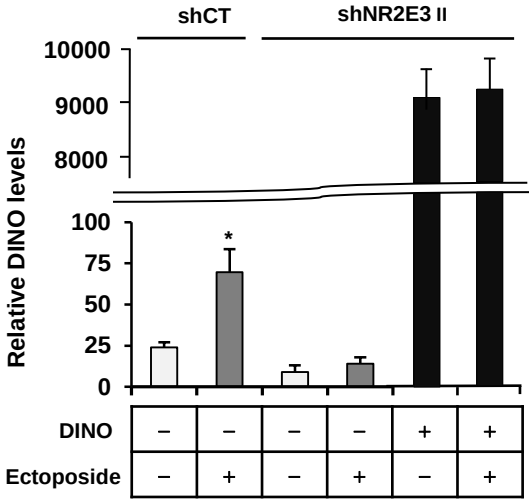

Supplementary Figure 9. DINO expression levels in control (shCT) HepG2 cells and NR2E3-depleted (shNR2E3 II) cells transfected with either empty vector or DINO expression plasmid.

A

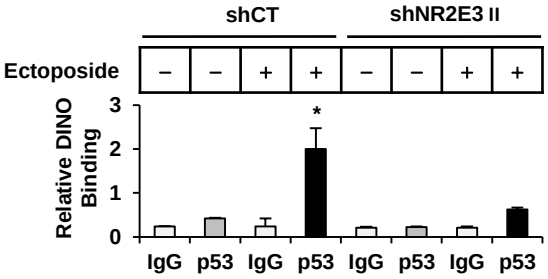

B

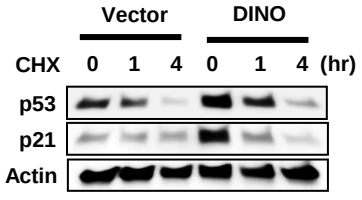

Supplementary Figure 10. A RIP-ChIP assay confirmed increased interaction between DINO and p53 in HepG2 control (shCT), not in NR2E3-depleted (shNR2E3 II). Cells were fixed after 4 hr etoposide treatment (A). HepG2 cells were transfected either with empty vector (vector) or DINO expression plasmid. DINO expression stabilizes p53 as shown by cycloheximide (CHX) chase analysis. p53 and p21 are shown at indicated time points after CHX addition (10 μg/ml) (B).

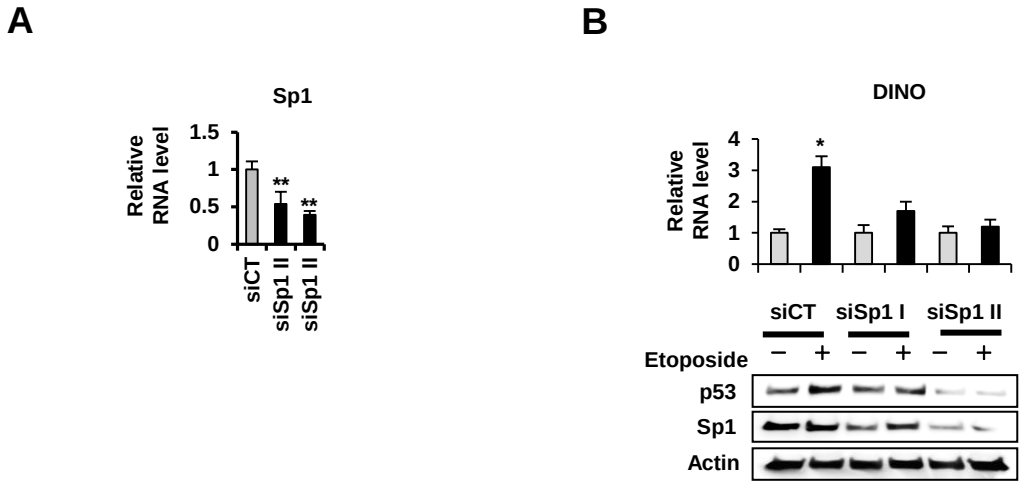

Supplementary Figure 11. Effects of Sp1 depletion on DINO induction and p53 activation. Sp1 proteins were depleted in HepG2 cells using small interfering RNAs targeting Sp1 (siSp1 I and II) with scrambled control (siCT). Sp1 depletion reduced Sp1 mRNA levels (A). The Sp1 depletion resulted in decreased DINO induction (B, top) and p53 activation (B, bottom). Values are represented as mean ± SD. *Significant induction or **repression $P < 0.05$.

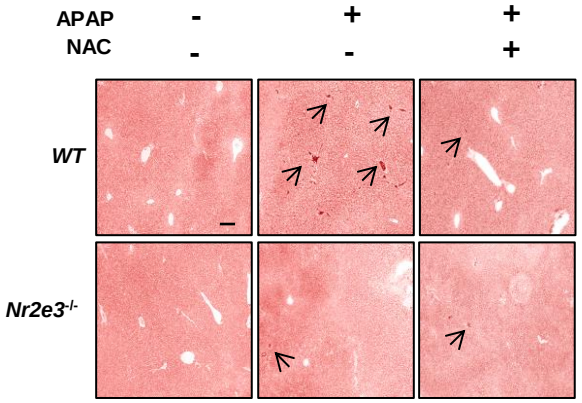

Supplementary Figure 12. Representative images of TUNEL-stained liver sections. Mice were treated first with APAP and then 90 min later with NAC. All tissues were collected 24 hr after APAP treatment. Black arrows indicate TUNEL-positive cells. Scale bar represents 100 μm.